Control of chaos by capture and release

John Starrett
Department of Mathematics, University of Colorado at Denver, Denver, Colorado 80211
(Received 16 July 2002; revised manuscript received 18 February 2003; published 28 May 2003)

We propose and demonstrate a different method for the control of flip saddles in dissipative chaotic systems. Due to the dynamics of a flip saddle, the stable manifolds of a target orbit and its perturbation can be modeled as a pair of concentric Möbius bands. Over the period of the target orbit, these bands rotate relative to one another. The method of capture and release (CR) takes advantage of this rotation, and captures a nearby system state in the perturbed stable manifold, releasing it when the rotation of the Möbius bands brings them into alignment. Unlike the method of Ott, Grebogi, and Yorke and most of its variants, CR does not rely on the unstable component of the flow to push the system state onto the stable manifold; the system state is evolving in a stable subspace for the duration of the control perturbation.

DOI: 10.1103/PhysRevE.67.056221 PACS number(s): 05.45.Gg

Since the 1990 paper of Ott, Grebogi, and Yorke (OGY) [1] on model independent chaos control, numerous simplifications, variations, and extensions have appeared. Overwhelmingly, these methods rely on the expanding part of the dynamics to push a system state onto the stable manifold of a target orbit, after which the contracting part draws it into the target. The low-dimensional control scheme proposed by Ott *et al.* spawned many variations. We now have control methods for high-dimensional systems [2–4], spatiotemporal systems [5–7], systems using time-delay coordinates [8,9], systems with multiple parameters [10,11], and systems with no accessible control parameter [12,13]. Most of these methods will work for simple saddles (eigenvalues greater than zero) and flip saddles (eigenvalues less than zero). An interesting subclass of these controllers relies on the nature of the flip saddle for their success. Because of the Möbius band structure of the manifolds associated with a flip saddle, the relationship of the perturbed and unperturbed manifolds during the course of an orbit is more complicated than that of a simple saddle.

Control methods relying on the nature of the flip saddle dynamics are for the most part realized in continuous time systems, and have been very successful in controlling physical systems [14–16], especially those where a model is unavailable and the location of periodic orbits is unknown. Pyragas [17] proposed a method (time-delayed autosynchronization) for continuous systems that synchronized the current state with the state delayed by one period, and Socolar *et al.* [18] improved on this method by including information about the system state over several previous cycles (extended time-delayed autosynchronization). The general method is known as time-delayed feedback [19–21].

A phase-space picture of a system state in the neighborhood of a flip orbit would reveal a roughly spiral path both approaching and departing the area of the saddle. Therefore, the distance s between a system state $\mathbf{x}(t)$ at time t and the state $\mathbf{x}(t-T)$ at time $t-T$, where T is the period of the target orbit, will decrease or increase depending on whether the system state is approaching or departing the neighborhood. An effective controller should decrease the level of perturbation as this distance diminishes, so we expect that the control perturbation $\delta\rho$ would be proportional to s. It is easy to see that time-delayed feedback relies on the alternating nature of a flip orbit.

In contrast to the continuous parameter dependence of time-delayed feedback on the distance from the system state to the target state, OGY-type controls apply a fixed control perturbation based on the measurement of the system state at a surface of section (SOS) map. Most OGY-type controls are two-step processes. In the first step, the system state is directed to the stable manifold of the target orbit using the unstable dynamics of a perturbation. In the second step, the controller is turned off and the system state evolves under the stable dynamics to the target. Whereas time-delayed feedback controls, like other OGY variants, rely on the dynamics of the unstable direction to nudge the system state onto the target orbit or its stable manifold, the method we propose, *capture and release* (CR), uses only the relative rotation of the stable manifolds of the perturbed and unperturbed orbits as the initial step to gain control.

I. BASIC GEOMETRY OF FLIP SADDLES

Flip orbits are continuous periodic saddle orbits whose local stable and unstable manifolds have an odd number of twists, so that at the surface of section the system state flips from one side to another of the stable and unstable manifolds. For a period-one orbit, these manifolds are Möbius bands. While in the strictest sense a Möbius band is $I\times S^1$, an interval crossed with a circle with a half twist, this method will work (with obvious modifications) on systems whose saddles have manifolds with one-half twist or more. Thus, nonflip saddle orbits whose manifolds undergo an even number of twists can also be controlled by our method. In this paper, however, all the analysis and control will be done on a period-one flip orbit.

II. ORGANIZATION OF THE PAPER

This paper is organized as follows. We examine the evolution of sets of perturbed manifolds of period-one flip orbits

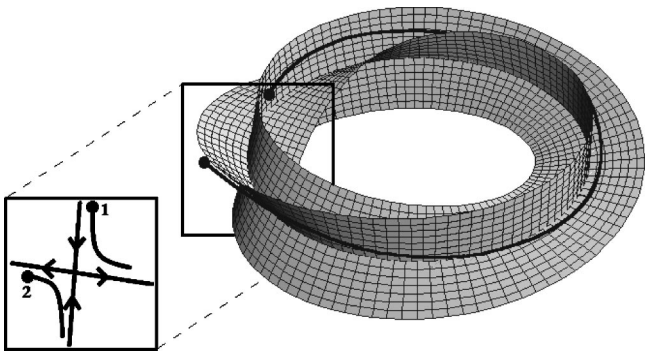

FIG. 1. The dynamics of a saddle orbit at the surface of section $(\mathrm{SOS})_{\phi(\tau)}$.

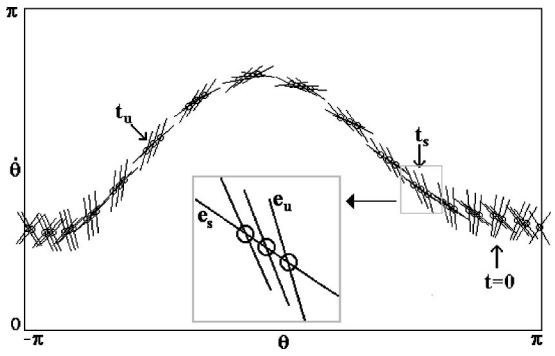

FIG. 2. Local stable and unstable manifolds of a period-one over-the-top orbit of the pendulum at 16 Poincaré sections for three levels of damping, $\rho=0.21$, $\rho=0.23$, and $\rho=0.25$. Each group of three consists of an unperturbed orbit (center) and two perturbations, corresponding to a greater or lesser damping. Units on the axes are in radians.

from data from a simulation of a parametrically driven pendulum and extract the relevant local manifold model: two offset pairs of intersecting Möbius bands. We then build a simple graphical tool that makes the dynamics near these sets of offset Möbius bands transparent. Using the simplified picture of the dynamics near a flip saddle, we design a control rule that uses only the stable dynamics of the local system, and finally demonstrate the control on a chaotic pendulum.

III. RESTRICTIONS, ASSUMPTIONS, AND SIMPLIFICATIONS

For simplicity, we will consider only periodically forced three-dimensional systems, so that the global flow will have a two-dimensional Poincaré section $\mathrm{SOS}_{\phi(t)}$ and a natural fundamental period T equal to that of the forcing $\phi(t)=\phi(t+T)$. Such a system lives naturally in a torus $P\times S^1$, where P is some phase space and S^1 is a circle. Consider a period-one orbit $\overline{\mathbf{x}}(t)=\overline{\mathbf{x}}(t+T)$ of such a system. As with all local control methods, the important geometric elements are the unperturbed target orbit $\overline{\mathbf{x}}$ along with its stable and unstable manifolds W_s, W_u, and the perturbed target orbit $\overline{\mathbf{x}}_{\rho(t)}$ along with its stable and unstable manifolds $W_s(\rho(t)), W_u(\rho(t))$. We assume the dynamics near the target orbit are linear so that at some reference Poincaré section $\mathrm{SOS}_0=\mathrm{SOS}_{\phi(t_0)}$, the unperturbed system is governed by a linear map $\mathbf{x}_{i+1}=A\mathbf{x}_i$, where A is a 2×2 matrix and $\mathbf{x}=\hat{\mathbf{x}}-\overline{\mathbf{x}}$ for $\hat{\mathbf{x}}$ some orbit near $\overline{\mathbf{x}}$. The perturbed system is governed by the linear map $\mathbf{x}_{i+1}-\delta\rho_i\mathbf{g}=A(\mathbf{x}_i-\delta\rho_i\mathbf{g})$, where $\delta\rho_i=\rho_i-\rho_0$ is a small perturbation of ρ and $\mathbf{g}=\partial\overline{\mathbf{x}}/\partial\rho$. For a linear system, the stable and unstable manifolds are approximated by the stable and unstable eigenvectors $\mathbf{e}_s, \mathbf{e}_u$ of the matrix A, and for a flip saddle their associated eigenvalues are $\lambda_u<-1<\lambda_s<0$. The mapping in the surface of section alternates sides of both the stable and unstable manifolds, as seen in the schematic of Fig. 1. For the full continuous orbit, the system state will flow along the hyperbolic leaves that foliate the crotch of the saddle, rotating by π each cycle of the orbit. Thus, as in the map, an orbit will return to its original ''quadrant'' every two cycles.

IV. THE PENDULUM MODEL

Figure 2 shows the perturbed and unperturbed eigenvectors of a period-one flip orbit from a simulation of a vertically forced pendulum with damping at 16 Poincaré phases $\mathrm{SOS}_0, \ldots, \mathrm{SOS}_{15}$ and at three different damping levels. The equation of motion is

$$\ddot{\theta}=\rho\dot{\theta}+\sin\theta(1-\alpha\cos(\omega t)),$$

where ρ is velocity dependent damping, θ is the angle measured counterclockwise from the straight down position, and α is the amplitude of the forcing. In our experiment, $\alpha=1.2$ and $\omega=1.5$.

The phase space is periodic at the left and right sides, forming an annular or cylindrical phase space, and only the upper half phase plane is shown in Fig. 2. The orbit moves from left to right. In each group of three, the middle manifolds are the unperturbed ones, with a damping level $\rho_0=0.23$ in dimensionless units of actual damping to small angle approximation critical damping. The left members of the trios are at an increased damping level $\rho=0.25$, and the right members have a damping of $\rho=0.21$. In the fifth full group of three from the left, the unstable manifolds are aligned, and in the eleventh group of three, the stable manifolds are aligned. This alignment of the unstable and stable manifolds is the heart of the method, and we will designate by t_u and t_s, respectively, the times at which these alignments take place. Due to the rotation by π of these manifolds over the course of an orbit, the evolution of the system in continuous time takes place near a pair of intersecting Möbius bands.

V. THE GEOMETRIC MODEL

To see more clearly the relation of the perturbed and unperturbed stable (or unstable) manifolds as pairs of Möbius bands, refer to Fig. 3, where we see the continuous evolution of two Möbius bands representing a pair of stable (or unstable) manifolds of a perturbed and unperturbed periodic orbit. Figure 3 shows a pair of perturbed stable manifolds, so

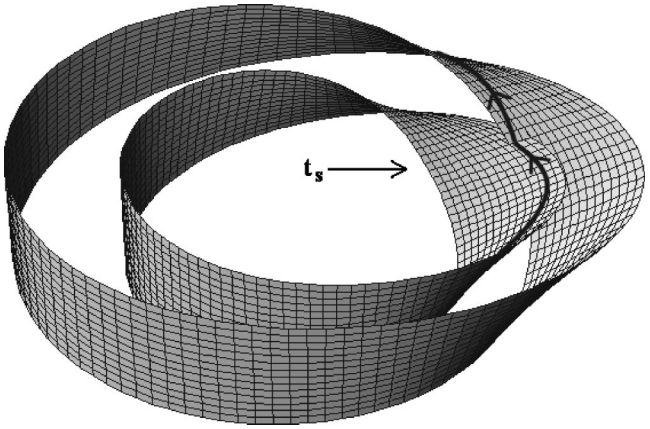

FIG. 3. A pair of perturbed Möbius bands. Because of their identical torsion, they are always parallel to each other. At one point, though, the bands are not just parallel, but they align as well, that is, their tangent planes are identical. The point at which the bands are most nearly aligned is labeled t_s. An orbit in the inner band is shown transferring to the outer band at t_s.

the point at which the bands are most nearly collinear in cross section is labeled t_s.

In order to visualize our control strategy, we consider the coevolving perturbed and unperturbed systems. Most of the details of the perturbed manifold structure and the dynamics of nearby orbits are irrelevant to CR control. In particular, the size of the eigenvalues is not important, although a larger stable eigenvalue λ_s will accelerate the convergence to the target orbit once the control is turned off. Likewise, the scissoring of the manifolds is unimportant, since the system state once captured in the stable perturbed manifold will evolve in it and be unaffected by the unstable dynamics. Therefore, we build a diagram with orthogonal manifolds, and a constant perturbation to get a simplified view of the dynamics of the perturbed and unperturbed saddles.

The manifold diagram of Fig. 4 shows the dynamics from the reference frame of the unperturbed manifolds. The stable manifold is fixed on the horizontal axis, and we imagine that the perturbed manifold structure orbits around it. This diagram is equivalent to one with both centers fixed and side by side with the manifolds rotating around the centers like propellers (as we would get by straightening the orbit in Fig. 4). In the reference frame of one of the bands, the other band makes an orbit every two fundamental system times, and

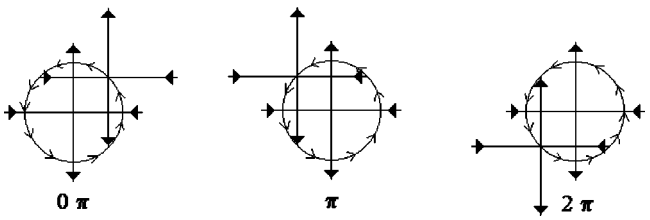

FIG. 4. Local manifolds rotating about one another are equivalent to manifolds that rotate about their centerlines but whose centerlines are fixed relative to each other. The labels beneath the figures refer to the distance around the torus that contains the attractor.

keeps the same orientation, i.e., the tangent vectors from the center manifold to the edges of the bands are almost parallel.

VI. THE METHOD

As with all OGY derived schemes, we rely on the ergodicity of the system to deliver a chaotic orbit to a controllable region surrounding the target orbit. Once the system state enters the controllable region, we perturb the system so that the system state lies in the stable manifold of the perturbed target orbit. From Fig. 3, it is apparent that any orbit lying in the stable manifold of the perturbed system will also lie in the (linear) stable manifold of the unperturbed system at time t_s. We may capture the system state at any time other than t_s, since at t_s the perturbation shifts the target orbit solely along the stable manifold $\mathbf{e}_s$. The time t_u is a good choice, because at this time the perturbation moves the target orbit solely along the unstable manifold. Assuming that t_u is our capture time, our goal is to find a $\delta\rho$ that will perturb the fixed point $\overline{\mathbf{x}}$ at time t_u by $\delta\rho\mathbf{g}$ so that the system state $\mathbf{x}$ lies in the perturbed stable manifold $\overline{\mathbf{x}}_\rho = \delta\rho\mathbf{g}$. This condition is satisfied when $\mathbf{f}_u \cdot (\mathbf{x} - \delta\rho\mathbf{g}) = 0$ or

$$\delta\rho = \frac{\mathbf{f}_u \cdot \mathbf{x}_n}{\mathbf{f}_u \cdot \mathbf{g}}, \tag{1}$$

where $\mathbf{f}_u$ is a vector orthogonal to the stable eigenvector $\mathbf{e}_s$. If we apply this correction $\delta\rho$, the phase point will be on the perturbed stable manifold until the correction is turned off at t_s. The system state $\mathbf{x}$ is now captured by the stable dynamics of the perturbed orbit. We leave the control on for a time $t_r = t_s - t_u$ until $\mathbf{x}$ lies in $\mathbf{e}_s$, the stable manifold of $\overline{\mathbf{x}}$. The control is turned off and the system state is released into $\mathbf{e}_s$. Again, refer to Fig. 3 to see the geometrical situation just before and just after time t_s. The system will now evolve along $\mathbf{e}_s$ to the target orbit. This process is illustrated diagrammatically in Fig. 5.

VII. DETERMINATION OF t_s

Capture and Release control depends in a critical way on the time t_s at which the perturbed and unperturbed stable manifolds coincide, so it is important to be able to make this determination. We assume that, as with OGY control, we are able to determine the perturbed and unperturbed local dynamics near the periodic orbit $\overline{\mathbf{x}}$ to be stabilized by computing the state transition matrix A for the local linear map $\mathbf{x}_{i+1} = A\mathbf{x}_i$. Then the eigenvectors $\mathbf{e}_s, \mathbf{e}_u$ of A approximate the local linear stable and unstable manifolds. Further, it must be possible to turn off the control perturbation at time t_s. There are several possible methods of making this determination, and we will mention them, but not go into too much detail.

A. Determination from sampled data

Ideally, we would like to have a system in which it is possible to sample the data at any time during the period of the orbit to be stabilized. In our simulation, and also in our physical pendulum system, we are able to take multiple

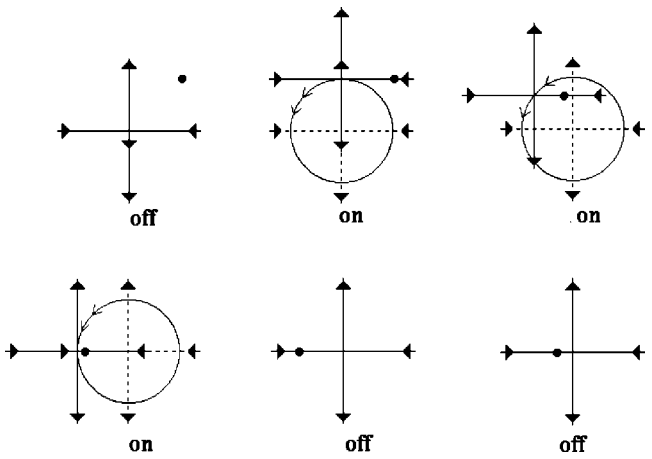

FIG. 5. Control by capture and release. The system state enters the controllable region, and a control perturbation is made that places the stable manifold on the system state. The system state then evolves in the perturbed stable manifold, while the perturbed manifold structure orbits around the unperturbed orbit. At time t_s, the stable manifolds are collinear, and the control is turned off. Thereafter, the system evolves toward the target orbit in the unperturbed stable manifold.

Poincaré sections and therefore, determine the time t_s from inspection of relative positions of the perturbed and unperturbed manifolds, or by minimizing $\mathbf{f}_u \cdot \mathbf{g}$ over the linear maps constructed at each Poincaré section. Then, if necessary, we can further refine our estimate of t_s by interpolation between the two times t_{s^+} and t_{s^-}, the two times that minimize $\mathbf{f}_u \cdot \mathbf{g}$. The ideal off time t_s is presumably between these two times. If necessary, new data could then be taken near time t_s and $\mathbf{f}_u \cdot \mathbf{g}$ checked to see if it is small enough. In practice, we found that visual data from the display shown in Fig. 2 was accurate enough.

B. Determination by the failure of OGY

OGY control depends on the dynamics in the unstable direction pushing the system state onto the stable manifold of the target orbit. If the system of interest is continuous then OGY control (or any other chaos control method that uses the unstable dynamics of the system) will fail if it is applied at a time t_s when the perturbation moves the target orbit entirely along the stable manifold. This condition means $\mathbf{f}_u \cdot \mathbf{g} = 0$, so $\delta\rho = \lambda_u/(\lambda_u - 1)\mathbf{f}_s \cdot \mathbf{x}/(\mathbf{f}_s \cdot \mathbf{g}) = \infty$, i.e., an infinite perturbation is required. Therefore, if a unique time t_s can be found for which OGY control is totally ineffective then that time will be the ideal off time t_s for CR.

C. Determination from a local model

If continuous data or closely spaced data from a close approach to the saddle is available, it is possible to make a local model in the form of a Floquet solution. The method of building this model from data is the subject of a paper in preparation. The Floquet solution is the product of an initial state vector and several time-varying matrices, one of whose columns consist of the (time-varying) eigenvectors that define the local linear manifolds of the saddle. The off time t_s can be found by solving $\mathbf{f}_u(t) \cdot \mathbf{g}(t) = 0$ for t using Newton's method.

VIII. RELATIONSHIP OF CR TO OGY

The method of Ott, Grebogi, and Yorke aims to control a system whose dynamics near a periodic orbit $\overline{\mathbf{x}}$ can be represented by a linear map $\mathbf{x}_{i+1} = A\mathbf{x}_i$. The system is controlled by making a perturbation $\delta\rho$ that places the system state's next iterate $\mathbf{x}_{i+1}$ in the stable manifold $\mathbf{e}_s$ of $\overline{\mathbf{x}}$. This condition is obtained when $\mathbf{f}_u \cdot \mathbf{x}_{i+1} = 0$, where $\mathbf{f}_u$ is perpendicular to $\mathbf{e}_s$. Therefore, the control rule for OGY is found by solving $\mathbf{f}_u \cdot \mathbf{x}_{i+1} = \mathbf{f}_u \cdot [A(\mathbf{x}_i - \delta\rho\mathbf{g}) + \delta\rho\mathbf{g}] = 0$ for $\delta\rho$.

If we wished to place the system state on the stable manifold after n iterates rather than one, we would solve

$$\mathbf{f}_u \cdot \mathbf{x}_{i+n} = \mathbf{f}_u \cdot [A^n(\mathbf{x}_i - \delta\rho\mathbf{g}) + \delta\rho\mathbf{g}] = 0. \tag{2}$$

In order to solve the system, we make use of the following relations:

$$\mathbf{f}_u \cdot \mathbf{e}_u = \mathbf{f}_s \cdot \mathbf{e}_s = 1,$$

$$\mathbf{f}_s \cdot \mathbf{e}_u = \mathbf{f}_u \cdot \mathbf{e}_s = 0,$$

or

$$\begin{bmatrix} \mathbf{f}_s^T \\ \mathbf{f}_u^T \end{bmatrix} [\mathbf{e}_s \mathbf{e}_u] = \begin{bmatrix} 1 & 0 \\ 0 & 1 \end{bmatrix}.$$

We can rewrite A as

$$A = [\mathbf{e}_u \mathbf{e}_s] \begin{bmatrix} \lambda_u & 0 \\ 0 & \lambda_s \end{bmatrix} \begin{bmatrix} \mathbf{f}_u^T \\ \mathbf{f}_s^T \end{bmatrix} = [\lambda_s \mathbf{e}_s \mathbf{f}_s^T + \lambda_u \mathbf{e}_u \mathbf{f}_u^T].$$

A^n is therefore equal to

$$[\mathbf{e}_u \mathbf{e}_s] \begin{bmatrix} \lambda_u^n & 0 \\ 0 & \lambda_s^n \end{bmatrix} \begin{bmatrix} \mathbf{f}_u^T \\ \mathbf{f}_s^T \end{bmatrix} = [\lambda_s^n \mathbf{e}_s \mathbf{f}_s^T + \lambda_u^n \mathbf{e}_u \mathbf{f}_u^T],$$

and we have, upon solving Eq. (2),

$$\delta\rho = \frac{\lambda_u^n}{\lambda_u^n - 1} \frac{\mathbf{f}_s \cdot \mathbf{x}}{\mathbf{f}_s \cdot \mathbf{g}}.$$

If we take the limit as $n \to \infty$, we get

$$\delta\rho = \lim_{n \to \infty} \frac{\lambda_u^n}{\lambda_u^n - 1} \frac{\mathbf{f}_s \cdot \mathbf{x}}{\mathbf{f}_s \cdot \mathbf{g}} = \frac{\mathbf{f}_s \cdot \mathbf{x}}{\mathbf{f}_s \cdot \mathbf{g}},$$

which is the CR rule.

Geometrically, the effect of delaying OGY control is to move the perturbed stable manifold closer to the current system state, so that it takes longer for the state to get from near the perturbed stable manifold to the unperturbed stable manifold. As we delay OGY control longer and longer, the perturbed stable manifold is moved closer and closer to the current system state, until, by delaying OGY control

indefinitely, we obtain the CR rule. If the perturbed and unperturbed stable manifolds did not cross, as they do with flip saddles, the captured system state could not be directed to the unperturbed stable manifold, and CR would not work.

IX. CONTROL OF A CHAOTIC PENDULUM

The forced pendulum is a popular ''test bed'' for chaos control schemes [22–28]. We applied the method of capture and release to our pendulum simulation and found it to be comparable to OGY control in terms of time to control and robustness to modeling errors (see Fig. 6). In this example, OGY control was found to require about 60% more ''energy'' than CR, where by energy we mean the integral of the perturbation over time. This was mainly due to CR control being off more than half the time by design. CR was found to be slightly more susceptible to instability due to noise than OGY, temporarily losing control, on an average, about once every 1000 iterates at a level of 0.1% additive noise, the level at which OGY is just able to keep uninterrupted control.

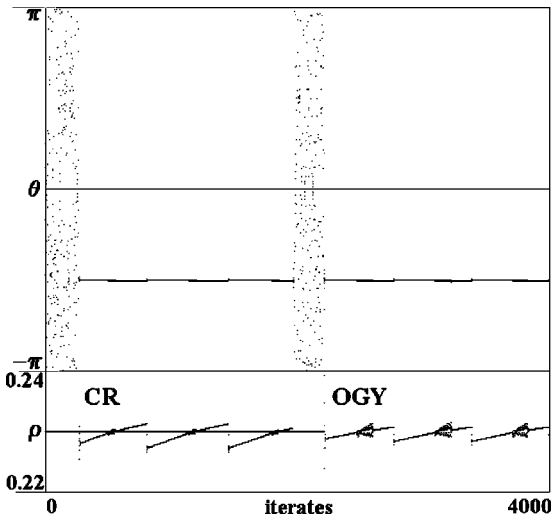

FIG. 6. Control of a period-one over-the-top orbit of the parametrically forced pendulum by CR and OGY. Small modeling errors have roughly the same effect on the nature of the controlled orbit for both OGY and CR.

X. SUMMARY

We have demonstrated a different control procedure for chaotic systems that relies in a fundamental way on the nature of the flip orbit. This method does not use the unstable dynamics of the system at all, but instead relies on the relative rotation of the perturbed and unperturbed stable manifolds to bring the system state to the stable manifold of the target orbit once it has been captured in the stable manifold of a perturbed orbit. As with OGY control, the perturbation is removed once the stable manifold is attained, allowing the system state evolve in the stable manifold to the target orbit. The method of capture and release has been found to be robust, and uses less energy to control than OGY in the system we tested. Because the unstable dynamics are not involved in the control, CR may be a good choice for systems with a large unstable component.

[1] C. Grebogi, E. Ott, and J.A. Yorke, Phys. Rev. Lett. **64**, 1 (1990).
[2] D. Auerbach, C. Grebogi, E. Ott, and J. Yorke, Phys. Rev. Lett. **69**, 3479 (1992).
[3] M. Yang, W. Ding, V. In, W.L. Ditto, M.L. Spano, and B. Gluckman, Phys. Rev. E **53**, 4334 (1996).
[4] D.L. Hill, Int. J. Bifurcation Chaos Appl. Sci. Eng. **11**, 1753 (2001).
[5] I. Aranson, J. Levine, and L. Tsimring, Phys. Rev. Lett. **72**, 2561 (1994).
[6] G. Hu, Z. Qu, and K. He, Int. J. Bifurcation Chaos Appl. Sci. Eng. **5**, 901 (1995).
[7] C. Lourenco, M. Hougardy, and A. Babloyantz, Phys. Rev. E **52**, 1528 (1995).
[8] U. Dressler and G. Nitsche, Phys. Rev. Lett. **68**, 1 (1992).
[9] J. Alvarez-Ramírez, R. Femat, and J. González, Phys. Lett. A **211**, 41 (1996).
[10] E. Barreto and C. Grebogi, Phys. Rev. E **52**, 3553 (1995).
[11] J. Warncke, M. Bauer, and W. Martienssen, Europhys. Lett. **25**, 323 (1994).
[12] A. Garfinkel, M.L. Spano, W.L. Ditto, and J.N. Weiss, Science (Washington, DC, U.S.) **257**, 1230 (1992).
[13] D.J. Christini and J.J. Collins, Phys. Rev. E **53**, R49 (1996).
[14] R. Roy, T.D. Murphy, Jr., T.D. Maier, Z. Gills, and E.R. Hunt, Phys. Rev. Lett. **68**, 1259 (1992).
[15] M.E. Bleich and J.E.S. Socolar, Phys. Rev. E **54**, 17 (1996).
[16] E.R. Hunt, Phys. Rev. Lett. **67**, 1953 (1991).
[17] K. Pyragas, Phys. Lett. A **170**, 421 (1992).
[18] J.E.S. Socolar, D.W. Sukow, and D.J. Gauthier, Phys. Rev. E **50**, 3245 (1994).
[19] C. Batlle, E. Fossas, and G. Olivar, Int. J. Circuit Theory Appl. **27**, 617 (1999).
[20] M.E. Brandt and G.R. Chen, Int. J. Bifurcation Chaos Appl. Sci. Eng. **10**, 2781 (2000).
[21] W. Just, in *Handbook of Chaos Control*, edited by H.G. Schuster (Wiley-VCh, New York, 1999).
[22] G.L. Baker, Am. J. Phys. **63**, 832 (1995).
[23] B. Hübinger, R. Doerner, and W. Martienssen, Z. Phys. B: Condens. Matter **90**, 103 (1993).
[24] S.R. Bishop and D. Xu, J. Sound Vib. **194**, 287 (1996).
[25] R.J. de Korte, J.C. Schouten, and C.M. van den Bleek, Phys. Rev. E **52**, 3358 (1995).
[26] N.J. Corron, S.D. Pethel, and B.A. Hopper, Phys. Rev. Lett. **84**, 3835 (2000).
[27] Z.H. Guan, G.R. Chen, and T. Ueta, IEEE Trans. Autom. Control **45**, 1724 (2000).
[28] K. Yagasaki and T. Uozumi, Int. J. Bifurcation Chaos Appl. Sci. Eng. **7**, 2827 (1997).